

Multiscale Modeling of Virus Structure, Assembly, and Dynamics

Eric R. May, Karunesh Arora, Ranjan V. Mannige, Hung D. Nguyen,
and Charles L. Brooks III

1 Introduction

Viruses are traditionally considered as infectious agents that attack cells and cause illnesses like AIDS, Influenza, Hepatitis, etc. However, recent advances have illustrated the potential for viruses to play positive roles for human health, instead of causing disease [1, 2]. For example, viruses can be employed for a variety of biomedical and biotechnological applications, including gene therapy [3], drug delivery [4], tumor targeting [5], and medical imaging [6]. Therefore, it is important to understand quantitatively how viruses operate such that they can be engineered in a predictive manner for beneficial roles.

Most viruses are nanosized particles that replicate only inside a host cell they infect. A structure of a complete virus particle is made up of a protective coat of protein called a capsid that encloses its nucleic acid, either DNA or RNA. Virus capsids are extremely stable and possess wide-ranging mechanical strengths, which can be characterized in the theoretical framework typically used for characterizing materials [7–9]. Capsids exhibit diversity in not only material properties but also geometric attributes. Capsids across the virosphere display a wide diversity of

E.R. May • K. Arora • C.L. Brooks III (✉)

Department of Chemistry and Biophysics Program, University of Michigan,
Ann Arbor, MI 48109, USA

e-mail: ericmay@umich.edu; karunesh@umich.edu; brookscsl@umich.edu

R.V. Mannige

Department of Chemistry and Chemical Biology, Harvard University, Cambridge,
MA 02138, USA

e-mail: ranjanmannige@gmail.com

H.D. Nguyen

Department of Chemical Engineering and Materials Science, University of California,
Irvine, Irvine, CA 92697, USA

e-mail: hdn@uci.edu

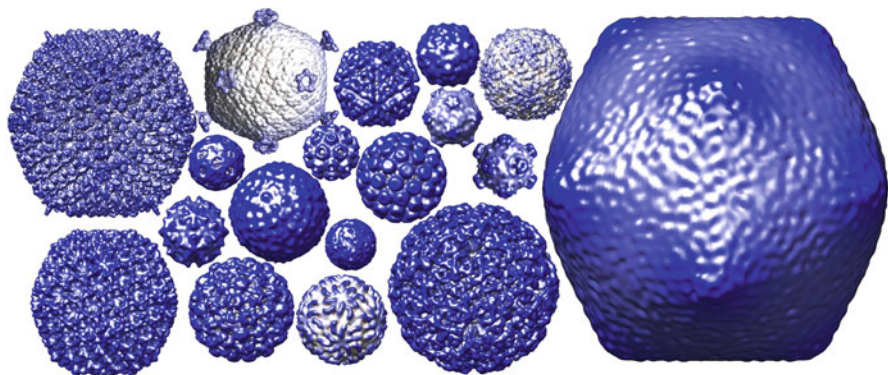


Fig. 1 As evident in the collage above, capsids come in a range of sizes (images represent electron microscopy reconstructions deposited into the virus particle explorer web site: viperdb.scripps.edu)

shapes, sizes, and architectures (Fig. 1), and understanding how these differences affect the material properties will provide design principles for engineering capsids.

Virus capsids are built from spontaneous self-assembly of multiple copies of a single protein or a few distinct proteins arranged in a highly symmetrical manner. Capsid assembly, from individual proteins in a correct, rapid, and spontaneous fashion on a biological timescale, is crucial for spreading an infection *in vivo* [10, 11]. Therefore, elucidating the means by which viral capsid self-assembly occurs may assist in the development of novel approaches to interfere with the assembly process and ultimately prevent viral infections. Following assembly, some virus capsids undergo morphological changes which are critical for the virus maturing into an infectious particle [12, 13]. Understanding the dynamic behavior of assembled capsids is equally essential to gain insight into the mechanism associated with the maturation process and may open avenues for rational drug design by providing clues for disrupting the maturation process.

Despite several experimental [14–17] and theoretical efforts [18–20], the underlying principles that govern virus capsid self-assembly and maturation are not well understood. Experimental approaches such as X-ray crystallography and cryo-electron microscopy have provided excellent starting points to begin understanding virus architecture in an intricate manner, but do not provide the dynamical information crucial for understanding the virus life cycle. Other experimental methods probing dynamical and mechanical properties of viruses still lack sufficient resolution in the length and timescales to decipher the movement of individual proteins constituting the virus capsid. Rapid increases in the availability of computer power and algorithmic advances have made possible simulations of complete viruses in atomic detail on the timescale of tens of nanoseconds [21, 22], which are providing some insights into the experiments just noted. However, atomically detailed simulation remains a considerable challenge, at increasingly large time and length scales, for processes of biological importance such as assembly and maturation of virus capsids.

We have applied multiscale computational approaches ranging from topology-based mathematical modeling to physical simulations at different levels of coarse graining to describe the underpinnings of virus function and structural organization. This chapter describes key findings of our group's work in elucidating the underlying principles that govern the assembly and maturation of virus capsids using state-of-the-art multiscale simulation approaches; our focus is on presenting insights gained by various multiscale approaches rather than simulation details, which can be found in individual papers. Following a brief introduction into virus architecture, we describe the biological findings from simple mathematical models concerning the optimal subunit shape for constructing a capsid and the origins of evolutionary discrimination of certain T -numbers. We then describe key results, from self-assembly simulations of virus capsids using coarse-grained modeling, related to the generalized mechanistic description of structural polymorphism often observed *in vitro*. Following, we describe the development of a true multiscale approach linking equilibrium atomic fluctuations with macroscopic elastic properties of virus capsids and apply this approach to investigate the buckling transitions of HK97 bacteriophage. We conclude by outlining future applications and required model developments.

2 Background on Spherical Virus Architecture

A sampling of spherical viruses is shown in Fig. 1 to illustrate the size and shape diversity of virus capsids. Understanding how these structures form, as well as the reasons behind the differences in shape and size of virus structures is fundamentally important. Let us set the stage by providing a brief and historical introduction to the architecture of spherical virus capsids. The foundations of modern structural virology began in the 1950s, in the days before high (subnanometer) resolution imaging was available. During that time, it was becoming clear that the size of any capsid was much larger than the largest protein that the enclosed viral genome could express. Crick and Watson reasoned that one could form such a capsid only if viruses figured out a way to arrange multiple copies of a smaller protein (a “sub”-unit) into the form of a shell. Based on rudimentary crystallographic evidence [23], Crick and Watson had proposed that the capsid would have to assume a high order symmetry group. In doing so, large copies of the same subunit (now known to be a single protein) would possess identical or equivalent positions within the capsid (hence the idea of equivalence between the subunits). The proposed symmetries were the ones displayed by platonic solids [24], of which, icosahedral symmetry, a 60-fold symmetry, is the highest in order. However, new methods (such as negative staining electron microscopy) soon showed that the number of subunits per capsid were in slight disagreement with the Crick–Watson proposal. It was observed that instead of an icosahedral structure with 60 equivalent subunits, spherical capsids, albeit icosahedrally symmetric, were found to be composed of multiples of 60 subunits.

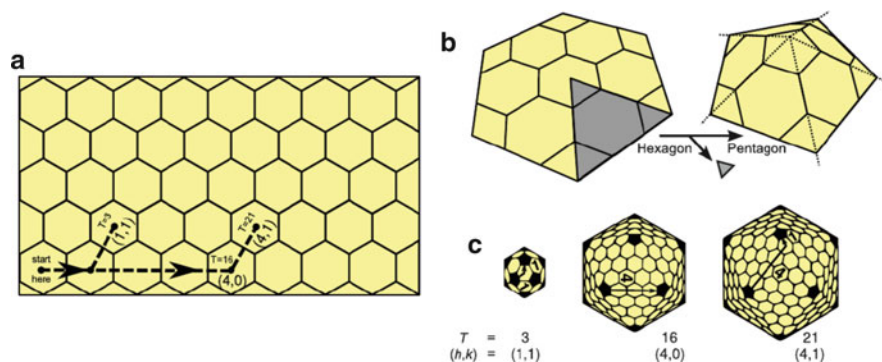


Fig. 2 Making capsid models of various sizes described by (h, k) pairs. The general idea is that all capsids consist of 12 pentamers (darkened in (c)) and a variable number of hexamers. Starting from only a sheet of hexagons (a), where hexagons represent hexamers, and then selectively converting specific hexamers into pentamers (b), a complete icosahedron may be constructed

Further advancement in the method of negative staining and electron microscopy led to the observation that capsids are shells formed from repeated pentagon and hexagon-like arrangements. From these early experiments, two groups of structural virologists, Horne and Wildy [25] and Caspar and Klug [26], found an interesting solution to the scalability problem. In particular, both groups recognized that virus capsids of practically any size could be created by combining 12 pentamers (symmetric clusters of five subunits) with a variable number of hexamers (symmetric clusters of six subunits). Caspar and Klug went further to describe a theoretical mechanism to “build an icosahedral capsid shell from a flat lattice of hexagons.”

As shown in Fig. 2, a specific capsid can be described by two integers, h and k , representing steps in the h or k direction, respectively. By taking an “ h, k walk” on the hexagonal surface (Fig. 2a), one ends up on a hexagon which is to be converted into a pentagon. These hexagons can be converted into pentagons by excising 1/6th of the selected hexagon and gluing the unpaired edges (Fig. 2b). When this procedure is repeated to make 12 such pentagons, one will be left with a three-dimensional model of a complete icosahedral capsid, where pentagons and hexagons represent pentamers and hexamers, respectively.

Although h and k are useful in understanding capsid size and arrangements of pentamers and hexamers, it is not always convenient to deal with two numbers as a descriptor. Conveniently, Caspar and Klug [26] re-introduced a useful descriptor (initially described by Goldberg in the 1940s), the triangulation number,

$$T = h^2 + k^2 + hk. \quad (1)$$

T is useful because it easily describes the number of subunits ($60T$) and hexamers ($10(T-1)$) in the capsid and the number of distinct symmetry environments present within the capsid (which is T itself). Today, the triangulation number is the ubiquitous descriptor of virus architecture.

3 Mathematical and Geometric Models for Describing Virus Phenomena

In this section, we explore how concepts borrowed from mathematics and geometry may help in understanding structural features of virus capsids. Using these simplistic models, we have addressed problems at various levels of capsid research, ranging from understanding what is the optimal subunit shape for constructing a capsid, to understanding the prevalence of certain T -number structures and the absence of others.

3.1 *The Canonical Capsid Model*

The utility of simplistic models, which do not account for the specific atomic level interactions (i.e., an all-atom force field) have been useful in explaining various capsid phenomena such as capsid self-assembly [27–33], capsid morphology [34–37], subunit stoichiometry [38–40], mechanical properties [41–43], and symmetry [37, 44]. We will be primarily discussing one such geometric model, the “canonical capsid,” that has served as a useful platform for the elucidation of capsid design principles [36, 37, 40].

The concept of the “canonical capsid,” which is a surprisingly simple construct, is defined as a polyhedron whose faces, each representing a subunit, must be identical in shape. This model is also known as a “monohedral tiling.” This simple model is useful because a large number of capsids found in nature can be represented as monohedral tilings [40]. In addition, these models can shed light on various physical properties of virus capsids that can be described as canonical.

3.2 *Prediction of the Optimal Subunit Shape*

Given the construct of the canonical capsid, a key question for investigation is which subunit shapes are permitted to exist within the confines of the canonical capsid. Using simple geometry and polyhedral rules [40], we have shown that canonical capsids can only accommodate *one* type of “prototile” (subunit design) consisting of five interacting edges. The bisected trapezoid (Fig. 3a) is one such acceptable prototile design. It is the same subunit shape that appears in all the natural capsids (Fig. 3b) we find to be represented by the canonical capsid model [40]. It has indeed been identified that many viruses share a common subunit protein fold (the double β -barrel), without sharing high sequence identity [45]. It is quite surprising that a simple canonical capsid model predicts such a ubiquitous shape found in viruses infecting almost all domains of life. Apparently, nature may be forcing viral capsid proteins into adopting this very special shape. It is tempting to conjecture that there is an overarching evolutionary pressure that may be acting on virus capsid’s design.

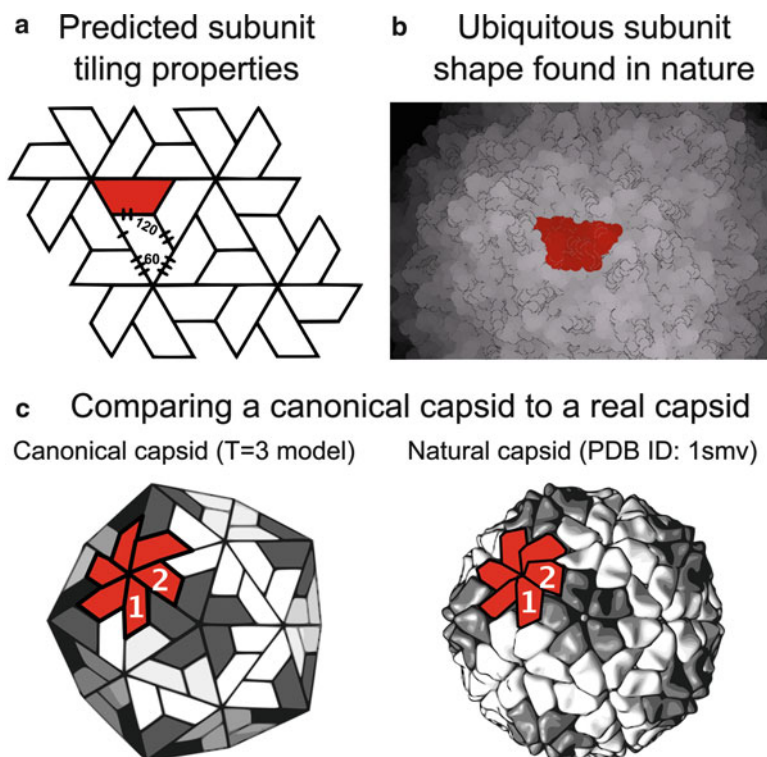
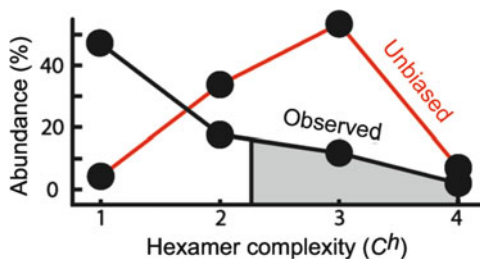


Fig. 3 *Canonical capsids as a model.* The basic subunit prototile—the bisected trapezoid (shaded in (a))—predicted from the analysis of the simplistic canonical capsid model [40] bears a strong resemblance to the subunit design ubiquitously found in virus capsids (b), indicating a mathematically motivated pressure in maintaining a trapezoidal subunit shape in nature. Apart from explaining the importance of the capsid subunit shape, the strong resemblance between these geometric entities and their real counterparts (exampled in (c)), allows for a number of studies in capsid design criteria [36,37]

3.3 Hexamer Complexity as a Predictor of Capsid Properties

Analysis of the virus structural data collected over the last half century indicates that a very large array of capsid sizes ranging from tens to many thousands of subunits are known to exist in nature (Fig. 1). However, some capsid sizes are rarer than others (such as $T = 12, 19$, and 27), an observation that has puzzled structural virologists as early as 1961 [25,26]. The cause for this apparent bias in the distribution of the observed capsid sizes is still not clearly understood. To explore if there is an evolutionary pressure that discriminates against certain capsid shapes, we further investigated intrasubunit interactions within virus capsids using a canonical capsid model. Specifically, we explored how subunits interact and how the angles between subunits can impose constraints on the capsid shape.

Fig. 4 As predicted by the inverse C^h rule, capsids with high hexamer complexity are underrepresented in nature as evident in the observed versus unbiased capsid abundances (% of families that display capsids of specific C^h)



The subunit–subunit angles present within the pentamers (which we call endo angles) impose constraints on the adjacent hexameric angles, an effect that is termed endo angle propagation [36]. While the shape and number of pentamers is fixed for all T number capsids, the number of hexamers (and therefore the shape) is not. The hexamers experience different environments based upon their adjacency to neighboring pentamers/hexamers. As a result, the angle patterns produced by interacting endo angles within the capsid ensure the emergence of three general morphological classes of capsids that can be differentiated by their h – k relationship [37]: *class 1* (described by the relationship $h > k = 0$), *class 2* ($h > k > 0$), and *class 3* ($h = k$). We have identified the minimum number of distinct hexamer shapes (which we call hexamer complexity C^h) required to form a canonical capsid of specific capsid size (T -number). Each canonical capsid of specific h and k is described by a single C^h value. Thus, C^h is very useful in systematically predicting properties of a group of capsids that were previously thought to be unrelated viruses.

C^h is also an indicator of the ease with which a capsid can be assembled, i.e., a larger number of distinct hexamer shapes would require a more complex assembly mechanism. Indeed, our modeling studies show that the capsids with a high C^h value require more auxiliary control mechanism for their assembly while the capsids with a low C^h value and low T – number ($T = 3, 4$, or 7) display the ability to assemble with no auxiliary requirements [46, 47]. Thus, the hexamer complexity number (C^h) can be used as tool to predict if a particular capsid assembly requires auxiliary mechanisms or proteins. Accordingly, we predicted that canonical capsids with larger C^h must be present with a lower frequency in nature since they require complex auxiliary assembly mechanisms. This hypothesis is corroborated by surveying all available capsid structures in the literature and virus structure databases. In the scenario that all T number capsids were equally probable, it would be expected that the complex capsids with $C^h > 2$ would represent the majority of the virus families observed in the nature (63%) (Fig. 4 *Unbiased*). However, in actuality, capsids with $C^h > 2$ represent only 5% of the observed capsid structures (Fig. 4 *Observed*). This suggests the existence of an evolutionary pressure which discriminates against viruses with a high hexamer complexity.

3.4 Limitations of the Canonical Capsid Model

A majority of the capsids we have studied display properties of canonical capsids [40]. However, the remaining small percentage of the noncanonical capsids cannot be well described by the canonical capsid model and likely require more sophisticated models for their characterization. For example, many noncanonical capsids possess nontrapezoidal subunit shapes (e.g., the members of the *polyomaviridae* family). It has been shown that these noncanonical capsids can be represented by other simplistic polyhedral models with slight embellishments [38, 39]. Still, there exist a few other noncanonical capsids with holes and large overlaps in their structures for which no simple solutions exist. It is these rule breakers that emphasize the requirement for more sophisticated theoretical models.

These mathematical modeling efforts have served to offer explanations to broad questions in the field of structural virology such as subunit shape and evolutionary discrimination of certain T -numbers. However, questions related to dynamical properties are more suitable to physics-based modeling studies. In the following sections, we will address two fundamental processes in the virus life cycle, capsid assembly (Sect. 4) and maturation (Sect. 5), using physics-based modeling techniques.

4 Self-Assembly of Virus Capsids

Highly specific and spontaneous self-assembly of individual proteins to form symmetric viral capsids inside the infected host cells is crucial for propagating the infection *in vivo* and is one of the most fundamental process of the virus life cycle. In addition, the *in vitro* self-assembly of empty capsids without the viral genome is of significant interest in bionanotechnology for vaccine design, gene therapy, and medical imaging [48]. As a specific example, empty capsids serve as vaccines to prevent cervical cancer, which is caused by the human papilloma virus. The vaccine, which consists of empty capsids of the human papilloma virus, prompts production of appropriate antibodies in the body, thereby priming an effective immune response that could be marshaled during subsequent exposure to the infectious virus [49]. The potency of the cervical vaccine depends strongly upon the degree of capsid self-assembly [50]. However, due to the inability to control assembly in laboratory and manufacturing practices, self-assembly of empty capsids often leads to architectural contaminants (i.e., structural polymorphism) [51]. A clear understanding of the kinetic mechanisms and thermodynamics of icosahedral capsid self-assembly would provide valuable insights into how to control the self-assembly process and is a key prerequisite to their widespread application in medicine.

The quantitative investigation of the virus capsid self-assembly mechanisms presents significant challenges for both experimental and computational approaches. Progress has been made toward understanding the molecular-level mechanisms

driving capsid formation through theoretical studies [19,20,38,44,52–55], structural analysis [56, 57], and *in vitro* self-assembly experiments of empty capsids using only purified capsid proteins [19,58,59]. Still, a detailed mechanistic understanding of the capsid self-assembly process is lacking. Despite rapid increases in the availability of computer power and algorithmic advances, atomically detailed simulations of the self-assembly process have been difficult due to the large system sizes and the long timescales involved in the process. As a consequence, to-date most simulation studies of capsid formation have been performed employing only simple coarse-grained models that significantly reduce the system size [32, 60, 61]. For example, Hagan and Chandler [32] modeled capsid proteins or capsomeres as point particles to simulate the assembly of small shells, Hicks and Henley [61] used an elastic model to represent capsid proteins as deformable triangles and Rapaport simulated the capsid self-assembly of polyhedra structures utilizing trapezoid units as a building block [28].

We investigated the spontaneous self-assembly process of different-sized virus capsids employing a coarse-grained molecular dynamics (MD) simulation approach. To increase the speed and efficiency of the simulations an extremely fast, event-driven method called discontinuous molecular dynamics (DMD) was employed [62–64]. Before performing simulations, we developed a range of geometric models that capture the geometric shape and energetic details of a coat protein without any specific built-in self-assembly rules such as nucleation. Interestingly, our prior two dimensional mathematical modeling studies, as well as, initial exploratory simulation studies by Rapaport [28] had predicted that the trapezoidal shape is a perfect building block to tile a closed icosahedral surface of any capsid size (see Sect. 3) [40]. To test this prediction by way of physical simulations, in our first generation of coat protein models each protein subunit was represented as a set of 24 beads arranged in four layers confined in the trapezoidal geometry (see Fig. 5a). Using a simplified model that exploits the important role of coat protein shape, together with the fast DMD method, allowed us to capture the spontaneous self-assembly of icosahedral capsids of different sizes as well as explore the optimal temperature and protein concentration required for the spontaneous self-assembly of capsids.

By performing over a hundred MD simulations at different temperatures and protein concentrations, we found that the assembly of $T = 1$ and $T = 3$ icosahedral capsids occurs with high fidelity only over a small range of temperatures and protein concentrations [33, 65]. Outside this range, particularly at low temperature or high protein concentration, large enclosed “monster particles” are produced (Fig. 5b). These mis-assemblies are remarkably similar to experimentally observed Turnip crinkle virus monster particles [66] or bacteriophage P22 monster particles [67]. Most importantly, our simulation studies revealed that the capsid assembly dynamics under optimal conditions is a nucleated process [58] involving monomer addition in which building blocks (either monomeric, dimeric, or trimeric species) are glued together in a sequential manner [33]. It is quite remarkable that our simulations employing simple models were able to recapitulate the experimental observations that capsid assembly is a nucleated process [19,58,59].

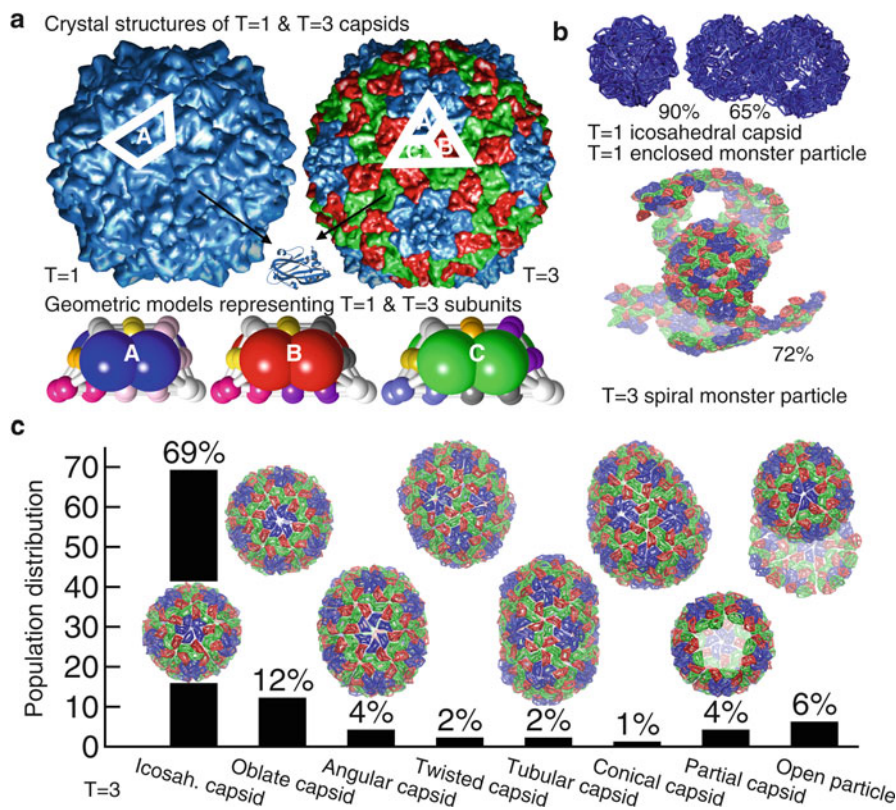


Fig. 5 (a) Coarse-grained models capturing the geometric shape of the protein and the protein-protein interactions that occur between proteins in the assembled capsid. (b) At low temperatures and high concentrations, assembly is nucleated too rapidly and partial growth leads to the combining of many partial capsids to form “monster particles” that are enclosed in $T = 1$ systems, and spiral-like in $T = 3$ systems, like those seen in cryo-EM experiments. (c) The assembly of $T = 3$ capsids under near optimal conditions yields a range of closed capsid forms that are determined by the number of five-to-six fold symmetry dislocations that occur as a result of certain kinetic pathways. The population distributions for supramolecular structures from $T = 3$ systems. The same structural polymorphism is also observed in $T = 1$ systems (Figures 1 and 2 of Nguyen et al. *J. Amer. Chem. Soc.*, 131:2606–14, 2009, copyright 2009, American Chemical Society.)

Interestingly, upon shifting the conditions (protein concentration and temperature) for $T = 1$ and $T = 3$ capsid growth slightly, we observed the self-assembly of not only icosahedral capsids, but also of a well-defined set of nonicosahedral yet completely enclosed and equally stable capsules [65] (Fig. 5c). These nonicosahedral capsules exhibit morphologies similar to particles that have been observed in the mis-assembly of capsids of many viruses [14, 68–74]. These findings demonstrate that structural polymorphism in capsid structure is an inherent property of capsid proteins, is independent of the morphology of constituent subunits, and arises from condition-dependent kinetic mechanisms that are determined by initial assembly conditions.

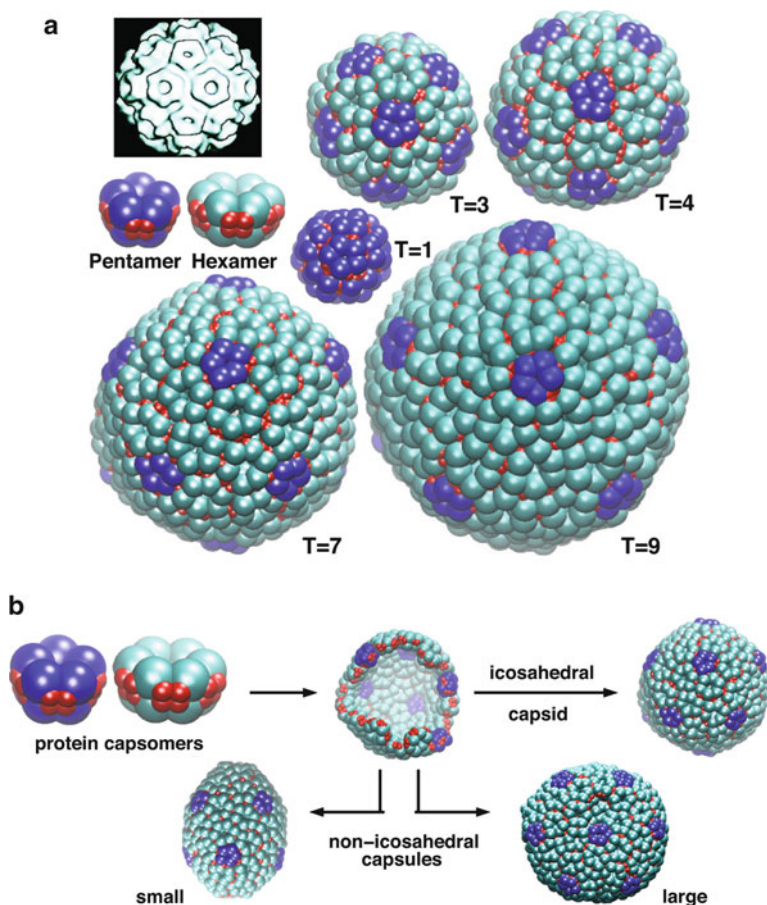


Fig. 6 (a) Coarse-grained model representing each pentameric or hexameric capsomer of coat proteins as a pentagonal or hexagonal structure for any T capsid systems, inspired by the presence of pentagonal and hexagonal morphology on many virus particles obtained from cryo-EM experiments. Each $T = 1, 3, 4, 7$, or 9 capsid obtained from our simulations contains 12 pentamers and $(T - 1)10$ hexamers arranged on icosahedral lattice. (b) Different kinetic mechanisms of assembly in $T = 7$ systems were deciphered: sequential addition for icosahedral capsids, condensation of preformed intermediates for large non-icosahedral capsules, and premature collapse of intermediates for small non-icosahedral capsules (Nguyen and Brooks, Nano Lett. 8: 4574–4581, 2008, copyright 2008, American Chemical Society.)

Considering the ubiquitous nature of nonicosahedral capsules observed in our simulations of $T = 1$ and $T = 3$ systems, we predicted that such capsules are also formed in $T > 3$ systems. We confirmed this prediction by developing our second generation of coarse-grained model in which multiples of coat proteins are represented as either pentameric or hexameric capsomers [75] (Fig. 6a). Our model capsomers mimic the building blocks of a few known virus systems such as HK97 capsids [76], which have been shown to assemble from pentamers and hexamers. In

the simulation studies of $T = 1, 3, 4, 7, 9, 12, 13, 16$, and 19 systems, we observed the formation of a variety of nonicosahedral yet highly ordered and enclosed capsules in addition to the expected icosahedral capsids. These simulations demonstrate that structural polymorphism is independent of the capsid complexity and the elementary kinetic mechanisms of self-assembly. Furthermore, the simulations revealed the existence of two distinctive and comprehensive classes of polymorphic structures. The first class includes aberrant capsules that are larger than their respective icosahedral capsids in $T = 1 - 7$ systems and the second class includes capsules that are smaller than their respective icosahedral capsids in $T = 7 - 19$ systems (Fig. 6b). The kinetic mechanisms responsible for the self-assembly of these two classes of aberrant structures were deciphered, providing insights into how to control the self-assembly of icosahedral capsids. To our knowledge, this is one of the first simulation studies that provided a generalized description of structural polymorphism, which is often observed in *in vitro* experiments [14, 68–70, 72, 73] and vaccine development studies [71].

Simulation studies, as described here, can provide new tools to inform potential strategies in antiviral development, protein design, and the engineering of novel biomaterials. The methodology employed in these studies could also be expanded upon to elucidate the means by which capsid proteins and the viral genome are self-assembled into full viruses. Such studies would enable us to make unique contributions to the field of virology/medicine by suggesting the development of novel ways to interfere with virus assembly and ultimately with viral infections.

5 Maturation and Mechanical Properties of Virus Capsids

An important aspect of designing nanotechnologies is material characterization; understanding how the material responds to stresses and different environmental conditions and ultimately the calculation of the fundamental mechanical moduli. Characterization of the mechanical properties of virus capsids is important for technology design as well as understanding the maturation phenomenon, which is one of the most fundamental process of the virus life cycle.

The $T = 7$ bacteriophage HK97 is a widely studied system [13, 76–81], due to its interesting structural features. This virus assembles into a procapsid structure consisting of 420 copies of a single protein and initially forms a rounded procapsid structure (Prohead II) as shown in Fig. 7 on the left. The seven protein asymmetric unit of Prohead II is also shown in Fig. 8. *In vivo* the structure matures upon packaging of the DNA genome, during which the structure expands, becomes faceted, and iso-peptide bonds form between side chains of different proteins, resulting in the mature (Head II) structure as shown in Fig. 7 on the right. The maturation transition (commonly termed a buckling transition) can also be triggered *in vitro* with empty capsids (genome deficient), by lowering the system pH [77, 82]. This maturation-related structural transition has broad implications for understanding virus behavior [83]. HK97 is believed to share many aspects of its maturation

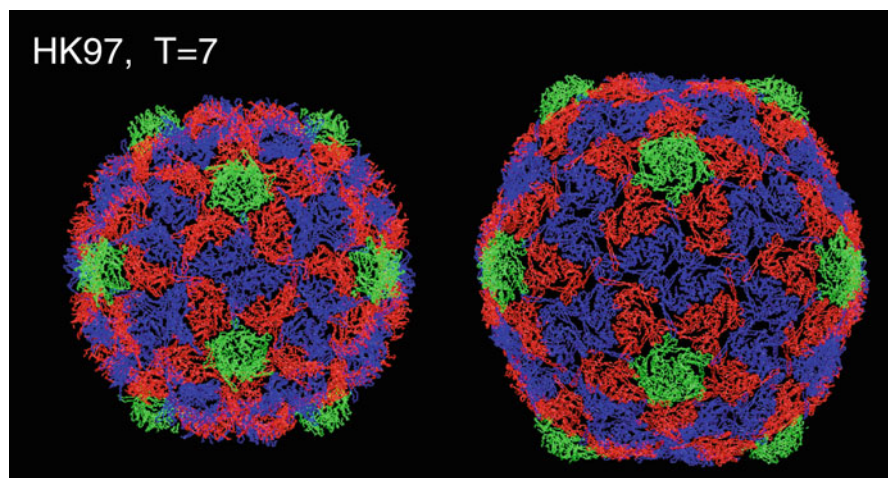


Fig. 7 The structures of HK97 ($T = 7$) in compact and swollen forms (Fig. 1 of Tama et al., J. Mol. Biol., 345: 299–314, 2005, copyright 2005 Elsevier B.V.)

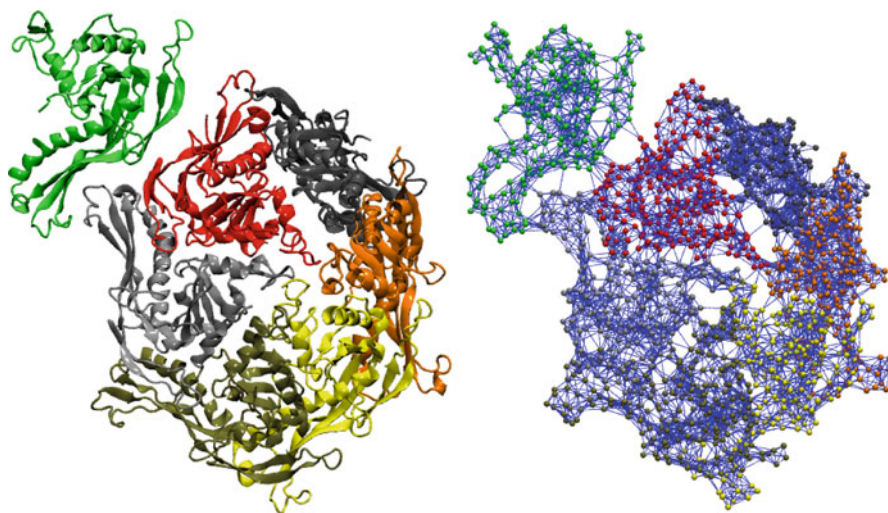


Fig. 8 The seven protein asymmetric unit of the virus HK97, represented with a ribbon drawing (*left*) and as an elastic network (*right*), in which the *lines* represent the harmonic springs of the network connecting C_α atoms within 8\AA of each other

process with other double-stranded DNA bacteriophages and with herpes virus [84]. Additionally, HK97 is an ideal system to understand what governs the equilibrium shape of spherical viruses because it exists in both a rounded (immature) and faceted (mature) forms during its life cycle. Understanding structural transitions of HK97 from a rounded to a faceted shape should help explain, in general, why certain

viruses adopt a particular configuration from the range of possible shapes and sizes (see Fig. 1).

Attempts to explain this faceting or buckling phenomena have been made using simplified models. Using the discrete canonical capsid model, we identified that viruses belonging to the *class 2* ($h > k > 0$) morphological group can undergo buckling transitions (See discussion in Sect. 3). The virus structures in this group, which includes HK97 ($T = 7$), have a degree of freedom associated with the hexamer configurations [36]. This is in contrast to the structures in *class 1* and *class 3* which we believe to consist of rigid hexamers, with zero degrees of freedom. This degree of freedom in the *class 2* hexamers was identified through our analysis of endo angle constraints (see Sect. 3), and we find two distinct stable states that the hexamer can sample. The two available hexamer configurations are a *pucker in* and *pucker out* state, corresponding to the faceted and rounded conformation of the capsid, respectively. An alternative explanation to the buckling phenomena has been put forth using purely continuum elastic theory of thin shells, proposed by Lidmar, Mirny, and Nelson (LMN) [41]. According to the LMN theory, the equilibrium configuration of the capsid is governed by a minimization of the elastic energy of the shell. As the elastic energy is dependent on the elastic properties of the shell, shape changes will arise in response to modulation of these properties. While both of these models have offered reasonable explanations for the buckling transition of virus capsids, neither work has incorporated molecular detail into their models. Recently, we have attempted to bridge the discrete and the continuum description of the virus capsid buckling transition by developing a multiscale approach which relates atomic level equilibrium fluctuations to the macroscopic elastic properties of the system [85, 86].

In the LMN theory, a single parameter, the Foppl-von Kármán number (γ), predicts whether a capsid will adopt a rounded or faceted form, and as can be seen in Fig. 1, both states are known to exist in nature. The shape dependence on γ is predicted to have a relatively sharp transition between rounded and faceted states, γ is given by

$$\gamma = \frac{Y R^2}{\kappa}, \quad (2)$$

where Y is the two-dimensional Young's modulus, R is the shell radius, and κ is the bending modulus. Determining Y and κ for capsid structures will allow γ to be determined, but it is inherently important to calculate these moduli to better understand the mechanical properties of these systems. Furthermore, the material characterization of capsids should accelerate the development of virus-based nanotechnologies.

It is difficult to measure the elastic properties of nano-sized objects such as virus capsids experimentally because most experimental techniques involve averaging over a large number of particles. However, the single-molecule technique of atomic force microscopy (AFM) is well suited for probing the mechanical strength of capsids through nanoindentation studies. These studies typically are conducted in conjunction with finite-element (FE) simulations in which the three-dimensional

Young's modulus (E) can be estimated by matching the AFM and FE force-displacement curves [87–91]. While these studies address how viruses respond to force loading, they do not directly evaluate the equilibrium mechanical properties of these systems. The loading rates in the AFM studies have been criticized for being too fast [42] and also the assumptions made in the finite element modeling that the capsid is an isotropic and homogenous medium may not be appropriate.

To overcome these limitations, we have developed a multiscale approach for calculating the continuum elastic properties Y and κ . In this approach, we utilize atomically detailed models to compute the equilibrium thermal fluctuations of the capsid, which are then related to the elastic properties of the capsid through an elastic Hamiltonian [85, 86]. The most relevant motions of the system, when trying to connect the atomic model to the continuum level theory, are the low frequency (long wavelength) collective motions. These collective motions arise from the atomic-level interactions and therefore a model is required which incorporates molecular detail. To compute collective motions, we utilize elastic network models (ENM), which incorporate molecular level details and variable density of interatomic interactions; an ENM representation of the asymmetric unit of HK97 is shown in Fig. 8 on the right. In addition, ENMs utilize a simple interaction potential which makes it computationally efficient to capture the collective motions of large macromolecular assemblies [92]. The essence of the ENM is that it is a harmonic approximation to the free energy minimum in which the structure lies. The numerous potential terms (Lennard–Jones, electrostatic, bond, angle, dihedral, etc) in a standard semi-empirical MD force field are replaced by a single harmonic potential term accounting for the vibrations of interacting pairs of atoms [93]. The normal modes of the ENM can be calculated by finding the eigenvectors of the Hessian matrix of second derivatives of the potential. A trajectory of the ENM can then be computed by propagating the network along a set of the lowest frequency normal modes.

From these ENM trajectories, a two-dimensional surface is computed by averaging over the shell thickness, and the fluctuations are projected onto a spherical harmonic basis set. The forces on a 2D elastic shell are known from the early works on continuum elastic theory of shells [94], and from these forces an energy density can be written down in the spherical harmonic basis. The total elastic energy can then be computed by integrating over the shell surface, which, due to the orthogonality properties of the basis set, reduces to a sum over the mode magnitudes

$$E = \frac{1}{2} \sum_l \left(8b + \kappa \frac{l(l-1)(l+1)(l+2)}{R^2} \right) |\hat{a}_l|^2, \quad (3)$$

where, $|\hat{a}_l|^2 \equiv \sum_{m=-l}^{+l} a_{lm} a_{lm}^*$, a_{lm} is the magnitude of spherical harmonic l, m , and b is the sum of the Lamé constants (λ, μ), from which Y can be calculated when a value for the Poisson ratio is known (or assumed). Given the quadratic form of the energy, the ensemble averages of $|\hat{a}_l|^2$ can be calculated and a relationship is obtained which contains only measurable surface properties ($R, \langle |\hat{a}_l|^2 \rangle$) and elastic

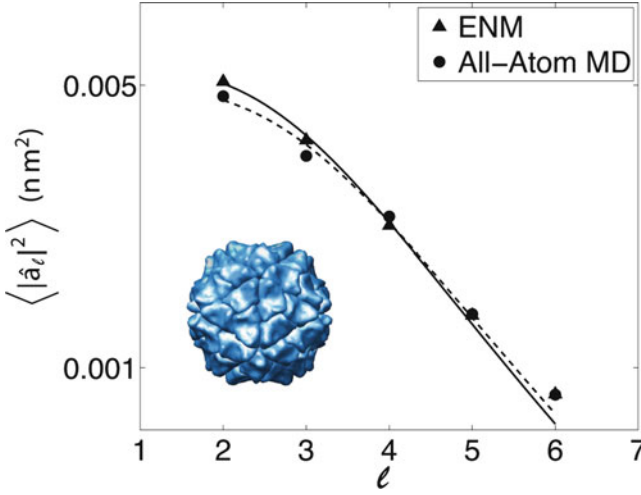


Fig. 9 The spectrum of spherical harmonics describing the equilibrium thermal fluctuations of the capsid surface for the $T = 1$ mutant of the *Sesbania mosaic virus*, shown in *bottom left*. A nearly identical spectrum is produced for an all-atom MD simulation of an entire capsid, as that from and elastic network model (ENM), that is scaled via an MD simulation of only the asymmetric unit. In both cases the fluctuation spectrum is well described by the theoretical model in (4) (Figure 1 of May and Brooks, Phys. Rev. Lett. 106:18801–18804, 2011, copyright, 2011 American Physical Society.)

parameters (λ, μ, κ)

$$\langle |\hat{a}_\ell|^2 \rangle = \frac{k_B T}{8b + \kappa \frac{l(l-1)(l+1)(l+2)}{R^2}}. \quad (4)$$

Our formulation of the ENM is a nondimensional model, and therefore we use MD to scale the trajectory to make it quantitatively accurate. The MD simulations are performed on the asymmetric unit of the capsid under icosahedral rotational boundary conditions [95]. From the MD simulations a scaling factor is calculated, which is passed to the ENM model to connect the cruder ENM model to the more accurate MD force field. We were able to show that this multiscale approach, combining an ENM with MD on the asymmetric unit, was a good approximation to the fluctuations generated by simulating the entire capsid explicitly with MD. The agreement between the theoretical model and the observed fluctuations, as well as the agreement between the multiscale (ENM) and the brute force MD approach are shown in Fig. 9. From the fits to the data, we are able to determine Y , κ , and γ for the $T = 1$ mutant of *Sesbania mosaic virus* (SeMV). We have applied this multiscale approach to HK97 [85, 86] in the mature and immature forms and predicted a significant change in γ (~ 200 immature, ~ 800 mature) between the states. These values are in agreement with the LMN theory, which predicts structures with $\gamma < 250$ should be spherical and those with higher γ values

should take on faceted forms, as is observed in Fig. 7. Additionally, we calculated a reduction in κ ($\sim 70 k_B T$ immature, $\sim 30 k_B T$ mature) between the states. This reduction in κ is functionally important, as it allows the faceted state, with the high curvature corners, to be adopted at a lower energy cost. Furthermore, it can be concluded from this analysis that the interactions which are changing during the transitions, function to reduce κ making the shell more flexible and enable it to reach the infectious state more efficiently. From this analysis we have inferred a mechanical mechanism for the maturation of HK97 by incorporating molecular details and have provided support for the LMN theory of buckling transitions. Further examination of larger ($T > 7$) capsid structures using this multiscale method will allow us to test our predictions from the canonical capsid model that only *class 2* capsids have the propensity to undergo buckling transitions.

6 Conclusions and Future Directions

We have studied several aspects of a virus capsid's behavior ranging from elastic properties to evolutionary pressures using a variety of modeling techniques. These techniques span the range from all-atom molecular simulations, to coarse-grained studies of assembly, to purely mathematical models. Clearly, maturation and capsid assembly, which are fundamental processes of virus life cycles span a wide range of spatial and temporal scales. To make progress, we have explored one virus life cycle process at a time, which allowed us to build models appropriate for the phenomena under investigation. Even within these independent studies, we have used multiscale approaches to bridge molecular level detail to continuum theory (Sect. 5), and incorporate what we learn at one level of description (*subunit shape*, Sect. 3), into our studies of other aspects of the life cycle (*assembly*, Sect. 4). The current work has offered explanations for several features of viruses not currently accessible through experimentation. The goal of all of these works is to gain a better understanding of how viruses operate and it is this knowledge that will further our ability to fight viral infections, develop and manufacture vaccines, and utilize capsids in nanotechnology applications. However, to have a greater impact on health and technology we must continue our exploration to elucidate the intricate and complex processes of virus life cycles.

In future studies, we will explore the transition pathways associated with structural changes of capsids. In an earlier study, normal mode analysis identified the dominant modes characterizing structural transitions of virus capsids, including HK97 [96]. In the case of HK97, two modes were required to describe the configurational change. Using these dominant icosahedral normal modes, pathways were constructed to connect the states of the system. However, these pathways may not be representative of the physical pathway the virus undergoes, because they are not refined against an “accurate” potential function. Computing the energetics of the pathway (free energy barriers, ΔG between stable states) requires using a more detailed potential. These calculations will require advanced sampling techniques to

“find” a minimal energy pathway and then compute the probabilities of the states along the path [97–99]. Understanding how pH effects the energetics of the pathway can also be incorporated into our pathway modeling efforts through constant pH-MD methods [100, 101]. The potential benefit of studying these transition pathways is that molecular interactions that have a drastic effect on the behavior of the system can be identified. For example, specific salt bridges might form at a given pH, but altering the pH could break those salt bridges and change the free energy barrier between the stable states. Identification of these key residues can be tested through mutagenesis studies, and could provide a target for preventing virus maturation. Similarly, the pathway methods can be combined with elasticity calculations such as described above, and residues that are responsible for altering the elastic character of the material can be identified. This knowledge could provide design principles for engineering novel capsids and for modulating the properties of capsids used in nanotechnologies. Understanding transition pathways is just one avenue of further investigation of viruses, other areas of interest include understanding viral protein–host protein interactions [102] and protein–nucleic acid interactions during virus assembly. Viruses have a rich array of features and phenomena that are still poorly understood. However, by building and employing computational and theoretical models that capture the essential physics of the underlying phenomenon, we can shed light on many of these unresolved aspects of the virus life cycle.

Acknowledgments This work has been supported by the NSF through the center for theoretical biological physics (CTBP) at the University of California, San Diego (PHY0216576), by the National Institute of Health for funding through the multiscale modeling tools for structural biology (MMTSB) research resource center RR012255, and research grant GM037555, and by the National Science Foundation through a postdoctoral fellowship to ERM (DBI-0905773).

References

1. Uchida, M., Klem, M.T., Allen, M., Suci, P., Flenniken, M., Gillitzer, E., Varpness, Z., Liepold, L.O., Young, M., Douglas, T.: Biological containers: protein cages as multifunctional nanoplateforms. *Adv. Mater.* **19**(8), 1025–1042 (2007)
2. Maham, A., Tang, Z., Wu, H., Wang, J., Lin, Y.: Protein-based nanomedicine platforms for drug delivery. *Small* **5**(15), 1706–1721 (2009)
3. Miller, A.D.: Human gene therapy comes of age. *Nature* **357**(6378), 455–460 (1992)
4. Douglas, T., Young, M.: Host-guest encapsulation of materials by assembled virus protein cages. *Nature* **393**(6681), 152–155 (1998)
5. Destito, G., Yeh, R., Rae, C.S., Finn, M.G., Manchester, M.: Folic acid-mediated targeting of cowpea mosaic virus particles to tumor cells. *Chem. Biol.* **14**(10), 1152–1162 (2007)
6. Gupta, S.S., Raja, K.S., Kaltgrad, E., Strable, E., Finn, M.G.: Virus-glycopolymer conjugates by copper(i) catalysis of atom transfer radical polymerization and azide-alkyne cycloaddition. *Chem. Commun. (Camb.)* (34), 4315–4317 (2005)
7. Smith, D.E., Tans, S.J., Smith, S.B., Grimes, S., Anderson, D.L., Bustamante, C.: The bacteriophage straight phi29 portal motor can package dna against a large internal force. *Nature* **413**(6857), 748–752 (2001)

8. Ivanovska, I., Wuite, G., Jansson, B., Evilevitch, A.: Internal dna pressure modifies stability of wt phage. *Proc. Natl. Acad. Sci. USA* **104**(23), 9603–9608 (2007)
9. Roos, W.H., Bruinsma, R., Wuite, G.J.L.: Physical virology. *Nature Phys.* **6**(10), 733–743 (2010)
10. Bancroft, J.B., Hills, G.J., Markham, R.: A study of the self-assembly process in a small spherical virus. Formation of organized structures from protein subunits in vitro. *Virology* **31**(2), 354–379 (1967)
11. Rose, R.C., Bonnez, W., Reichman, R.C., Garcea, R.L.: Expression of human papillomavirus type 11 (HPV-11) protein in insect cells: in vivo and in vitro assembly of viruslike particles. *J. Virol.* **67**(4), 1936–1944 (1993)
12. Conway, J.F., Duda, R.L., Cheng, N., Hendrix, R.W., Steven, A.C.: Proteolytic and conformational control of virus capsid maturation: the bacteriophage hk97 system. *J. Mol. Biol.* **253**(1), 86–99 (1995)
13. Lata, R., Conway, J.F., Cheng, N., Duda, R.L., Hendrix, R.W., Wikoff, W.R., Johnson, J.E., Tsuruta, H., Steven, A.C.: Maturation dynamics of a viral capsid: visualization of transitional intermediate states. *Cell* **100**(2), 253–263 (2000)
14. Adolph, K.W., Butler, P.J.: Studies on the assembly of a spherical plant virus. I. States of aggregation of the isolated protein. *J. Mol. Biol.* **88**(2), 327–41 (1974)
15. Rossmann, M.G.: Constraints on the assembly of spherical virus particles. *Virology* **134**(1), 1–11 (1984)
16. Ceres, P., Zlotnick, A.: Weak protein–protein interactions are sufficient to drive assembly of hepatitis b virus capsids. *Biochemistry* **41**, 11525–11531 (2002)
17. Johnson, J.M., Willits, D.A., Young, M.J., Zlotnick, A.: Interaction with capsid protein alters rna structure and the pathway for in vitro assembly of cowpea chlorotic mottle virus. *J. Mol. Biol.* **335**(2), 455–64 (2004)
18. Schwartz, R., Shor, P.W., Prevelige, P.E., Berger, B.: Local rules simulation of the kinetics of virus capsid self-assembly. *Biophys. J.* **75**, 2626–2636 (1998)
19. Zlotnick, A., Johnson, J.M., Wingfield, P.W., Stahl, S.J., Endres, D.: A theoretical model successfully identifies features of hepatitis b virus capsid assembly. *Biochemistry* **38**(44), 14644–14652 (1999)
20. Bruinsma, R.F., Gelbart, W.M., Reguera, D., Rudnick, J., Zandi, R.: Viral self-assembly as a thermodynamic process. *Phys. Rev. Lett.* **90**(24), 248101 (2003)
21. Arkhipov, A., Freddolino, P.L., Schulten, K.: Stability and dynamics of virus capsids described by coarse-grained modeling. *Structure* **14**(12), 1767–1777 (2006)
22. Zink, M., Grubmüller, H.: Mechanical properties of the icosahedral shell of southern bean mosaic virus: a molecular dynamics study. *Biophys. J.* **96**(4), 1350–1363 (2009)
23. Caspar, D.L.D.: Structure of bushy stunt virus. *Nature* **177**(4506), 476–477 (1956)
24. Crick, F.H., Watson, J.D.: Structure of small viruses. *Nature* **177**(4506), 473–475 (1956)
25. Horne, R.W., Wildy, P.: Symmetry in virus architecture. *Virology* **15**, 348–373 (1961)
26. Caspar, D.L., Klug, A.: Physical principles in the construction of regular viruses. *Cold Spring Harb. Symp. Quant. Biol.* **27**, 1–24 (1962)
27. Schwartz, R.S., Garcea, R.L., Berger, B.: ‘local rules’ theory applied to polyomavirus polymorphic capsid assemblies. *Virology* **268**(2), 461–470 (2000)
28. Rapaport, D.C.: Self-assembly of polyhedral shells: a molecular dynamics study. *Phys. Rev. E* **70**(5), 1539–1555 (2004)
29. Endres, D., Miyahara, M., Moisan, P., Zlotnick, A.: A reaction landscape identifies the intermediates critical for self-assembly of virus capsids and other polyhedral structures. *Prot. Sci.* **14**, 1518–1525 (2005)
30. Keef, T., Taormina, A., Twarock, R.: Assembly models for papovaviridae based on tiling theory. *Phys. Biol.* **2**(3), 175–188 (2005)
31. Keef, T., Micheletti, C., Twarock, R.: Master equation approach to the assembly of viral capsids. *J. Theor. Biol.* **242**(3), 713–721 (2006)
32. Hagan, M.F., Chandler, D.: Dynamic pathways for viral capsid assembly. *Biophys. J.* **91**, 42–54 (2006)

33. Nguyen, H.D., Reddy, V.S., Brooks III, C.L. Deciphering the kinetic mechanism of spontaneous self-assembly of icosahedral capsids. *Nano Lett.* **7**(2), 338–344 (2007)
34. Workum, K.V., Douglas, J.F.: Symmetry, equivalence, and molecular self-assembly. *Phys. Rev. E* **73**, 031502 (2006)
35. Chen, T., Zhang, Z., Glotzer, S.C.: A precise packing sequence for self-assembled convex structures. *Proc. Natl. Acad. Sci. USA* **104**(3), 717–722 (2007)
36. Mannige, R.V., Brooks III, C.L.: Geometric considerations in virus capsid size specificity, auxiliary requirements, and buckling. *Proc. Natl. Acad. Sci. USA* **106**(21), 8531–8536 (2009)
37. Mannige, R.V., Brooks III, C.L.: Periodic table of virus capsids: implications for natural selection and design. *PLoS One* **5**(3), e9423 (2010)
38. Twarock, R.: A tiling approach to virus capsid assembly explaining a structural puzzle in virology. *J. Theor. Biol.* **226**(4), 477–482 (2004)
39. Twarock, R.: Mathematical virology: a novel approach to the structure and assembly of viruses. *Phil. Trans. R. Soc. A* **364**, 3357–3373 (2006)
40. Mannige, R.V., Brooks III, C.L.: Tiling nature of virus capsids and the role of topological constraints in natural capsid design. *Phys. Rev. E* **77**(5), 051902 (2008)
41. Lidmar, J., Mirny, L., Nelson, D.R.: Virus shapes and buckling transitions in spherical shells. *Phys. Rev. E* **68**, 051910–051919 (2003)
42. Nguyen, T.T., Bruinsma, R.F., Gelbart, W.M.: Elasticity theory and shape transitions of viral shells. *Phys. Rev. E Stat. Nonlin. Soft. Matter Phys.* **72**(5 Pt 1), 051923 (2005)
43. Zandi, R., Reguera, D.: Mechanical properties of viral capsids. *Phys. Rev. E Stat. Nonlin. Soft. Matter Phys.* **72**, 021917 (2005)
44. Zandi, R., Reguera, D., Bruinsma, R.F., Gelbart, W.M., Rudnick, J.: Origin of icosahedral symmetry in viruses. *Proc. Natl. Acad. Sci. USA* **101**(44), 15556–15560 (2004)
45. Bamford, D.H., Grimes, J.M., Stuart, D.I.: What does structure tell us about virus evolution? *Curr. Opin. Struct. Biol.* **15**(6), 655–663 (2005)
46. Johnson, J.E., Speir, J.A.: Quasi-equivalent viruses: a paradigm for protein assemblies. *J. Mol. Biol.* **269**(5), 665–75 (1997)
47. Dokland, T., McKenna, R., Ilag, L.L., Bowman, B.R., Incardona, N.L., Fane, B.A., Rossmann, M.G.: Structure of a viral procapsid with molecular scaffolding. *Nature* **389**(6648), 308–313 (1997)
48. Douglas, T., Young, M.: Viruses: making friends with old foes. *Science* **312**(5775), 873–875 (2006)
49. Koutsky, L.A., Ault, K.A., Wheeler, C.M., Brown, D.R., Barr, E., Alvarez, F.B., Chiacchierini, L.M., Jansen, K.U.: A controlled trial of a human papillomavirus type 16 vaccine. *N. Engl. J. Med.* **347**(21), 1645–1651 (2002)
50. Shank-Retzlaff, M., Wang, F., Morley, T., Anderson, C., Hamm, M., Brown, M., Rowland, K., Pancari, G., Zorman, J., Lowe, R., Schultz, L., Teyral, J., Capen, R., Oswald, C.B., Wang, Y., Washabaugh, M., Jansen, K., Sitrin, R.: Correlation between mouse potency and in vitro relative potency for human papillomavirus type 16 virus-like particles and gardasil vaccine samples. *Hum. Vaccin.* **1**(5), 191–7 (2005)
51. Shi, L., Sings, H.L., Bryan, J.T., Wang, B., Wang, Y., Mach, H., Kosinski, M., Washabaugh, M.W., Sitrin, R., Barr, E.: Gardasil: prophylactic human papillomavirus vaccine development—from bench top to bed-side. *Clin. Pharmacol. Ther.* **81**(2), 259–64 (2007)
52. Wales, D.J.: Closed-shell structures and the building game. *Chem. Phys. Lett.* **141**, 478–484 (1987)
53. Berger, B., Shor, P.W., Tucker-Kellogg, L., King, J.: Local rule-based theory of virus shell assembly. *Proc. Natl. Acad. Sci. USA* **91**, 7732–7736 (1994)
54. Zlotnick, A.: To build a virus capsid. An equilibrium model of the self assembly of polyhedral protein complexes. *J. Mol. Biol.* **241**(1), 59–67 (1994)
55. Endres, D., Zlotnick, A.: Model-based analysis of assembly kinetics for virus capsids or other spherical polymers. *Biophys. J.* **83**, 1217–1230 (2002)

56. Reddy, V.S., Giesing, H.A., Morton, R.T., Kumar, A., Post, C.B., Brooks III, C.L., Johnson, J.E.: Energetics of quasiequivalence: computational analysis of protein-protein interactions in icosahedral viruses. *Biophys. J.* **74**(1), 546–558 (1998)
57. Shepherd, C.M., Borelli, I.A., Lander, G., Natarajan, P., Siddavanahalli, V., Bajaj, C., Johnson, J.E., Brooks III, C.L., Reddy, V.S.: Viperdb: a relational database for structural virology. *Nucleic Acids Res.* **34**, D386–D389. (2006)
58. Zlotnick, A., Aldrich, R., Johnson, J.M., Ceres, P., Young, M.J.: Mechanism of capsid assembly for an icosahedral plant virus. *Virology* **277**, 450–456 (2000)
59. Casini, G.L., Graham, D., Heine, D., Garcea, R.L., Wu, D.L.: In vitro papillomavirus capsid assembly analyzed by light scattering. *Virology* **325**, 320–327 (2004)
60. Zhang, T., Schwartz, R.: Simulation study of the contribution of oligomer/oligomer binding to capsid assembly kinetics. *Biophys. J.* **90**, 57–64 (2006)
61. Hicks, S.D., Henley, C.L.: Irreversible growth model for virus capsid assembly. *Phys. Rev. E Stat. Nonlin. Soft. Matter Phys.* **74**(3 Pt 1), 031912 (2006)
62. Alder, B.J., Wainwright, T.E.: Studies in molecular dynamics. I. General method. *J. Chem. Phys.* **31**, 459–466 (1959)
63. Rapaport, D.C.: Molecular dynamics simulation of polymer chains with excluded volume. *J. Phys. A* **11**, L213–L217 (1978)
64. Bellemans, A., Orban, J., Belle, D.V.: Molecular dynamics of rigid and non-rigid necklaces of hard discs. *Mol. Phys.* **39**, 781–782 (1980)
65. Nguyen, H.D., Reddy, V.S., Brooks III, C.L.: Invariant polymorphism in virus capsid assembly. *J. Am. Chem. Soc.* **131**(7), 2606–14 (2009)
66. Sorger, P.K., Stockley, P.G., Harrison, S.C.: Structure and assembly of turnip crinkle virus. ii. mechanism of reassembly in vitro. *J. Mol. Biol.* **191**(4), 639–658 (1986)
67. Earnshaw, W., King, J.: Structure of phage p22 coat protein aggregates formed in the absence of the scaffolding protein. *J. Mol. Biol.* **126**, 721–747 (1978)
68. Bancroft, J.B., Bracker, C.E., Wagner, G.W.: Structures derived from cowpea chlorotic mottle and brome mosaic virus protein. *Virology* **38**(2), 324–35 (1969)
69. Salunke, D.M., Caspar, D.L., Garcea, R.L.: Polymorphism in the assembly of polyomavirus capsid protein vp1. *Biophys. J.* **56**(5), 887–900 (1989)
70. Kanesashi, S.N., Ishizu, K., Kawano, M.A., Han, S.I., Tomita, S., Watanabe, H., Kataoka, K., Handa, H.: Simian virus 40 vp1 capsid protein forms polymorphic assemblies in vitro. *J. Gen. Virol.* **84**(Pt 7), 1899–905 (2003)
71. Zhao, Q., Guo, H.H., Wang, Y., Washabaugh, M.W., Sitrit, R.D.: Visualization of discrete 11 oligomers in human papillomavirus 16 virus-like particles by gel electrophoresis with coomassie staining. *J. Virol. Methods* **127**(2), 133–40 (2005)
72. Fu, C.Y., Morais, M.C., Battisti, A.J., Rossmann, M.G., Jr. Prevelige, P.E.: Molecular dissection of o29 scaffolding protein function in an in vitro assembly system. *J. Mol. Biol.* **366**(4), 1161–1173 (2007)
73. Dong, X.F., Natarajan, P., Tihova, M., Johnson, J.E., Schneemann, A.: Particle polymorphism caused by deletion of a peptide molecular switch in a quasiequivalent icosahedral virus. *J. Virol.* **72**(7), 6024–6033 (1998)
74. Cusack, S., Oostergetel, G.T., Krijgsman, P.C., Mellema, J.E.: Structure of the top a-t component of alfalfa mosaic virus. A non-icosahedral virion. *J. Mol. Biol.* **171**(2), 139–55 (1983)
75. Nguyen, H.D., Brooks III, C.L.: Generalized structural polymorphism in self-assembled viral particles. *Nano Lett.* **8**, 4574–81 (2008)
76. Xie, Z., Hendrix, R.W.: Assembly in vitro of bacteriophage hk97 proheads. *J. Mol. Biol.* **253**(1), 74–85 (1995)
77. Duda, R.L., Hempel, J., Michel, H., Shabanowitz, J., Hunt, D., Hendrix, R.W.: Structural transitions during bacteriophage hk97 head assembly. *J. Mol. Biol.* **247**(4), 618–635 (1995)
78. Wikoff, W.R., Liljas, L., Duda, R.L., Tsuruta, H., Hendrix, R.W., Johnson, J.E.: Topologically linked protein rings in the bacteriophage hk97 capsid. *Science* **289**(5487), 2129–2133 (2000)

79. Conway, J.F., Wikoff, W.R., Cheng, N., Duda, R.L., Hendrix, R.W., Johnson, J.E., Steven, A.C.: Virus maturation involving large subunit rotations and local refolding. *Science* **292**(5517), 744–748 (2001)
80. Ross, P.D., Conway, J.F., Cheng, N., Dierkes, L., Firek, B.A., Hendrix, R.W., Steven, A.C., Duda, R.L.: A free energy cascade with locks drives assembly and maturation of bacteriophage hk97 capsid. *J. Mol. Biol.* **364**(3), 512–525 (2006)
81. Gertsman, I., Gan, L., Guttman, M., Lee, K., Speir, J.A., Duda, R.L., Hendrix, R.W., Komives, E.A., Johnson, J.E.: An unexpected twist in viral capsid maturation. *Nature* **458**(7238), 646–650 (2009)
82. Gan, L., Conway, J.F., Firek, B.A., Cheng, N., Hendrix, R.W., Steven, A.C., Johnson, J.E., Duda, R.L.: Control of crosslinking by quaternary structure changes during bacteriophage hk97 maturation. *Mol. Cell* **14**(5), 559–569 (2004)
83. Steven, A.C., Heymann, J.B., Cheng, N., Trus, B.L., Conway, J.F.: Virus maturation: dynamics and mechanism of a stabilizing structural transition that leads to infectivity. *Curr. Opin. Struct. Biol.* **15**(2), 227–236 (2005)
84. Lee, K.K., Gan, L., Tsuruta, H., Hendrix, R.W., Duda, R.L., Johnson, J.E.: Evidence that a local refolding event triggers maturation of hk97 bacteriophage capsid. *J. Mol. Biol.* **340**(3), 419–433 (2004)
85. May, E.R., Brooks III, C.L.: Determination of viral capsid elastic properties from equilibrium thermal fluctuations. *Phys. Rev. Lett.* **106**, 188101–188104 (2011)
86. May, E.R., Aggarwal, A., Klug, W.S., Brooks III, C.L.: Viral capsid equilibrium dynamics reveals nonuniform elastic properties. *Biophys. J.* **100**, L59–L61 (2011)
87. Ivanovska, I.L., de Pablo, P.J., Ibarra, B., Sgalari, G., MacKintosh, F.C., Carrascosa, J.L., Schmidt, C.F., Wuite, G.J.L.: Bacteriophage capsids: tough nanoshells with complex elastic properties. *Proc. Natl. Acad. Sci. USA* **101**(20), 7600–7605 (2004)
88. Michel, J.P., Ivanovska, I.L., Gibbons, M.M., Klug, W.S., Knobler, C.M., Wuite, G.J.L., Schmidt, C.F.: Nanoindentation studies of full and empty viral capsids and the effects of capsid protein mutations on elasticity and strength. *Proc. Natl. Acad. Sci. USA* **103**(16), 6184–6189 (2006)
89. Kol, N., Gladnikoff, M., Barlam, D., Shneck, R.Z., Rein, A., Rousso, I.: Mechanical properties of murine leukemia virus particles: effect of maturation. *Biophys. J.* **91**(2), 767–774 (2006)
90. Carrasco, C., Carreira, A., Schaap, I.A.T., Serena, P.A., Gmez-Herrero, J., Mateu, M.G., de Pablo, P.J.: Dna-mediated anisotropic mechanical reinforcement of a virus. *Proc. Natl. Acad. Sci. USA* **103**(37), 13706–13711 (2006)
91. Roos, W.H., Gibbons, M.M., Arkhipov, A., Uetrecht, C., Watts, N.R., Wingfield, P.T., Steven, A.C., Heck, A.J.R., Schulten, K., Klug, W.S., Wuite, G.J.L.: Squeezing protein shells: how continuum elastic models, molecular dynamics simulations, and experiments coalesce at the nanoscale. *Biophys. J.* **99**(4), 1175–1181 (2010)
92. Tama, F., Brooks, C.L.: Symmetry, form, and shape: guiding principles for robustness in macromolecular machines. *Annu. Rev. Biophys. Biomol. Struct.* **35**, 115–133 (2006)
93. Tirion, M.M.: Large amplitude elastic motions in proteins from a single-parameter, atomic analysis. *Phys. Rev. Lett.* **77**(9), 1905–1908 (1996)
94. Landau, L.D., Lifshitz, E.M.: *Theory of Elasticity*. Pergamon Press, London (1959)
95. Cagin, T., Holder, M., Pettitt, B.M.: A method for modeling icosahedral virions rotational symmetry boundary-conditions. *J. Comput. Chem.* **12**(5), 627–634 (1991)
96. Tama, F., Brooks III, C.L.: Diversity and identity of mechanical properties of icosahedral viral capsids studied with elastic network normal mode analysis. *J. Mol. Biol.* **345**(2), 299–314 (2005)
97. Khavrutskii, I.V., Arora, K., Brooks III, C.L.: Harmonic fourier beads method for studying rare events on rugged energy surfaces. *J. Chem. Phys.* **125**(17), 174108 (2006)
98. Arora, K., Brooks III, C.L.: Large-scale allosteric conformational transitions of adenylate kinase appear to involve a population-shift mechanism. *Proc. Natl. Acad. Sci. USA* **104**(47), 18496–18501 (2007)

99. Arora, K., Brooks III, C.L. Functionally important conformations of the met20 loop in dihydrofolate reductase are populated by rapid thermal fluctuations. *J. Am. Chem. Soc.* **131**, 5642–5647 (2009)
100. Lee, M.S., Salsbury, F.R., Brooks III, C.L. Constant-pH molecular dynamics using continuous titration coordinates. *Proteins* **56**(4), 738–752 (2004)
101. Khandogin, J., Brooks III, C.L. Constant pH molecular dynamics with proton tautomerism. *Biophys. J.* **89**(1), 141–157 (2005)
102. May, E.R., Armen, R.S., Mannan, A.M., Brooks III, C.L.: The flexible c-terminal arm of the lassa arenavirus z-protein mediates interactions with multiple binding partners. *Proteins* **78**(10), 2251–2264 (2010)